September 25, 2008

Negative index metamaterials based on metal-dielectric nanocomposites for imaging applications

L. Menon
Northeastern University

W. T. Lu
Northeastern University

A. L. Friedman
Northeastern University

S. P. Bennett
Northeastern University

D. Heiman
Northeastern University

See next page for additional authors

AIP | Applied Physics Letters

Negative index metamaterials based on metal-dielectric nanocomposites for imaging applications

L. Menon, W. T. Lu, A. L. Friedman, S. P. Bennett, D. Heiman et al.

Citation: Appl. Phys. Lett. **93**, 123117 (2008); doi: 10.1063/1.2945647
View online: http://dx.doi.org/10.1063/1.2945647
View Table of Contents: http://apl.aip.org/resource/1/APPLAB/v93/i12
Published by the American Institute of Physics.

Negative index metamaterials based on metal-dielectric nanocomposites for imaging applications

L. Menon,[a] W. T. Lu,[b] A. L. Friedman, S. P. Bennett, D. Heiman, and S. Sridhar[c]
Department of Physics, Northeastern University, Boston, Massachusetts 02115, USA

(Received 7 February 2008; accepted 18 May 2008; published online 25 September 2008)

Negative index metamaterials are demonstrated based on metal-dielectric nanocomposites prepared using a versatile bottom-up nanofabrication approach. The method involves the incorporation of vertically aligned metal nanowires such as Au and Ag inside dielectric aluminum oxide nanotemplates. Optical absorbance measurements show resonance peaks corresponding to the transverse and longitudinal surface plasmon modes. A quantitative model based on effective medium theory is in excellent agreement with experimental data, and points to specific composite configurations and wavelength regimes where such structures can have applications as negative refraction media for imaging. © *2008 American Institute of Physics*. [DOI: 10.1063/1.2945647]

The development of next-generation optical devices such as flat lens and superlenses currently hinge on the demonstration of nanocomposite materials which will exhibit negative refraction in the optical wavelength regime.[1] Recent advances in nanofabrication both bottom up and top down clearly point to the feasibility of developing nanocomposites in various configurations in the near future which will indeed exhibit the required negative index of refraction. Particularly promising in this regard is the demonstration of nonlinear optical properties derived from surface plasmon modes exhibited in metal nanoparticles such as Au and Ag.[2–6] Combining such metal nanoparticles with dielectrics and fabricating them appropriately in novel configurations can produce structures which will exhibit negative index of refraction in specific visible wavelength regimes. Several such structures are currently being proposed.[7–11]

In this paper, we show that a metal nanowire array, such as Au or Ag, embedded vertically in a dielectric medium, such as aluminum oxide (see Fig. 1), can exhibit negative refraction in the visible wavelength regime. Consider such a metal nanowire array embedded in a dielectric medium. For such a material, if f is the ratio of metal wire versus dielectric (fill ratio), κ=measure of the aspect ratio of nanowires, ε_a=permittivity of the dielectric, ε_m=permittivity of the wires and ε_{eff}=effective permittivity of composite structure, then using effective medium theory,[12,13] one can write

$$0 = f\frac{\varepsilon_m - \varepsilon_{\text{eff}}}{\varepsilon_m + \kappa\varepsilon_{\text{eff}}} + (1-f)\frac{\varepsilon_a - \varepsilon_{\text{eff}}}{\varepsilon_a + \kappa\varepsilon_{\text{eff}}}. \quad (1)$$

For this equation, one has the solution $\varepsilon_{\text{eff}}(\kappa) = (\Delta \pm \sqrt{\Delta^2 + 4\kappa\varepsilon_a\varepsilon_m})/2\kappa$ with $\Delta = f(1+\kappa)(\varepsilon_m - \varepsilon_a) + \kappa\varepsilon_a - \varepsilon_m$. The $\pm$ sign is appropriately chosen to allow for positive values of the effective permittivity. The transverse and longitudinal components of the effective permittivity are $\varepsilon_\perp = \varepsilon_{\text{eff}}(\kappa)$ with $\kappa \sim 1$ and $\varepsilon_\parallel = \varepsilon_{\text{eff}}(\kappa)$ with $\kappa \gg 1$. In the ideal case of perfectly aligned nanowires, one has $\varepsilon_\perp = \varepsilon_{\text{eff}}(1) = \varepsilon_a\varepsilon_m/[f\varepsilon_a + (1-f)\varepsilon_m]$ and $\varepsilon_\parallel = \varepsilon_{\text{eff}}(\infty) = f\varepsilon_m + (1-f)\varepsilon_a$. From these expressions, it can be shown that there is a minimum $f_{\min} = \varepsilon_a/(\varepsilon_a - \text{Re}\,\varepsilon_m)$. For $f > f_{\min}$, $\text{Re}\,\varepsilon_\parallel < 0$ and for $f > \frac{1}{2}$, $\text{Re}\,\varepsilon_\perp < 0$. One can determine the fill conditions at which either $\text{Re}\,\varepsilon_\parallel < 0$ or $\text{Re}\,\varepsilon_\perp < 0$. The minimum fill ratio $f_{\min}$ corresponds with a specific λ_1, where $\text{Re}\,\varepsilon_\parallel = 0$. This λ_1 is the longitudinal plasmon resonance which according to the Drude model is strongly dependent on fill ratio. This model clearly predicts that for long wavelengths $\lambda > \lambda_\perp$, the medium behaves like an indefinite index medium[14] with $\text{Re}\,\varepsilon_\parallel < 0$ and $\text{Re}\,\varepsilon_\perp > 0$. As shown in (Ref. 11), such a medium can be used as a superlens.

To demonstrate such a negative index metamaterial, we have used a versatile bottom-up nanofabrication approach to prepare a high-aspect ratio metal nanowire array embedded in a dielectric aluminum oxide matrix. Such a metal-dielectric nanocomposite structure exhibits both longitudinal and transverse surface plasmon resonance modes in the absorbance as demonstrated in optical transmission measurements. The peak intensity and position of the resonances are found to depend strongly on nanocomposite parameters, incident polarization, and incident angle, consistent with modeling results based on the effective medium theory. Negative refraction and superlens imaging can eventually be realized in such structures in either parallel or perpendicular orientations of the incident radiation with respect to axis of the nanowires.[11] However, specific wavelength regimes are dictated by the position of the plasmon modes. Specifically, for large aspect ratio, length/diameter $\sim 10^3$, of the nanowires and small filling factors, (metal volume)/(dielectric volume) $\sim 10^{-1}$, negative refraction can occur at visible and near-infrared wavelengths. Structures with such parameters are easily constructed using the present nanofabrication approach.

The nanowires are synthesized inside nanoporous aluminum oxide films making a uniform array of vertical nanowires arranged parallel to each other. The fabrication method allows for the preparation of nanowires with small diameters ($d \leqslant 10$ nm) and large lengths ($l > 2$ μm), in effect, nanowires with large aspect ratio ($l/d \sim 10^3$). The optical absorbance is calculated from transmission measurements. The optical absorbance can be modeled by taking into account the plasmonic interaction between the metal nanowire and the aluminum oxide, where the filling factor of the metal inside the dielectric aluminum oxide and the aspect ratio of the nanowires are the main fitting parameters.

[a]Electronic mail: l.menon@neu.edu.
[b]Electronic mail: w.lu.@neu.edu.
[c]Electronic mail: s.sridhar@neu.edu.

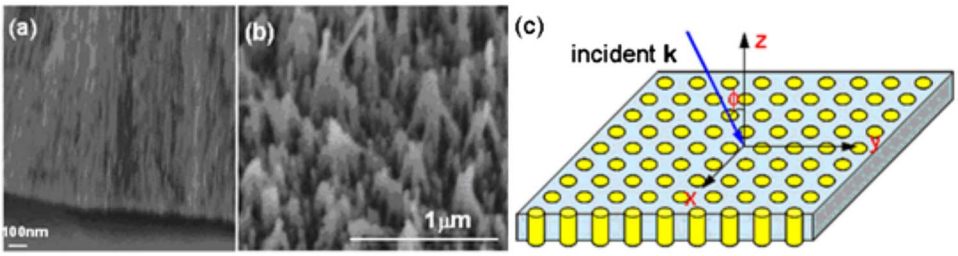

FIG. 1. (Color online) Scanning electron microscopy (SEM) image showing Au nanowires with diameter 10–12 nm (a) embedded inside alumina and (b) sticking out of the alumina. In (b) the SEM image was obtained by etching the template at the surface. In the actual templates used in this work, the wires remain embedded inside alumina. (c) Modeling of a typical nanowire-in-dielectric nanocomposite.

Nanoporous aluminum oxide templates are first generated by dc anodization of commercially available Al foil in an acidic electrolyte.[15] The pore diameter of the templates can be controlled by adjusting the fabrication parameters—most importantly the acid used and the applied dc voltage. In this work, templates with two different pore diameters were fabricated. Templates with pore diameter ~12 nm were fabricated by anodization in 15% sulfuric acid at 10 V and templates with pore diameter ~35 nm were fabricated by anodization in 3% oxalic acid at 40 V. The pore patterns are quasiordered and uniform. The time of anodization was adjusted to produce templates with large thickness (and correspondingly large pore lengths) ~4 μm. Below the porous layer is a thin barrier layer of aluminum oxide (approximately tens of nanometers) followed by the remaining unanodized aluminum. The nanowires are synthesized inside the templates by means of ac electrodeposition (20 V, 250 Hz).[6,16] In the case of Au, an aqueous solution consisting of $HAuCl_4$ (1 g/l) and boric acid (4 g/l) was used as electrolyte. For Ag nanowires, an aqueous solution containing $AgNO_3$ (1 g/l) was used as electrolyte. The unanodized Al layer below the pores was removed in mercuric chloride solution. This leaves behind a dielectric template consisting of embedded Au or Ag nanowires. Figure 1 shows typical scanning electron microscopy images of aluminum oxide membrane consisting of ~12 nm pores filled with Au wires. From the information on the wire dimensions and the pore parameters, the fill factors (ratio of metal versus dielectric) were calculated for the samples. For the wires with diameter 12 nm, the fill ratio ~0.05 while for the wires with diameter 35 nm, the fill ratio is ~0.20. Such templates demonstrate optical properties which have direct applications in negative refraction, as discussed below.

Transmission spectra for the nanowires with diameter 12 nm are shown in Figs. 2 (for Ag nanowires) and 3 (for Au nanowires) for varying angles of incidence with respect to the long-axis of the nanowires. The spectra were obtained over the wavelength range 300–1600 nm for varying angles of incidence (φ) for both *P*- and *S*-polarized waves. For the *P*-polarized (*S*-polarized) wave, the magnetic (electric) field is perpendicular to the wire axis. A Si photodetector was used for the lower wavelength regime, 300–1000 nm while an InGaAs photodetector was used for the higher wavelength regime, 1000–1600 nm. The optical absorbance, −ln(T), was computed from the optical transmission (T). The calculated absorbance as a function of wavelength are also shown in Figs. 2 and 3.

The important experimental results are now discussed. For Ag nanowires, the transmission for *S*-polarized light has a minimum at ~390 nm, shown in Fig. 2(a) for 12 ± 2 nm diameter wires. This corresponds to an absorbance peak seen in Fig. 2(b) arising from the transverse plasmon mode. This transverse-related feature appears for all angles of incidence. For this *S* polarization, the longitudinal plasmon mode is absent at longer wavelength. On the other hand, the *P*-polarized spectra show a clear absorbance peak for the longitudinal plasmon at 845 nm. The peak is absent at normal incidence but is observed to become prominent for increasing angles of incidence. The interaction of the *P*-polarized wave with the nanocomposite at small angles of incidence (close to the normal) is similar to the interaction of the *S*-polarized wave with the nanocomposite at all angles of incidence. This is expected since under these conditions the polarization axis is perpendicular to the axis of the nanowires and hence the two polarization directions are equivalent. For *S*-polarized waves, the nanocomposite medium is isotropic

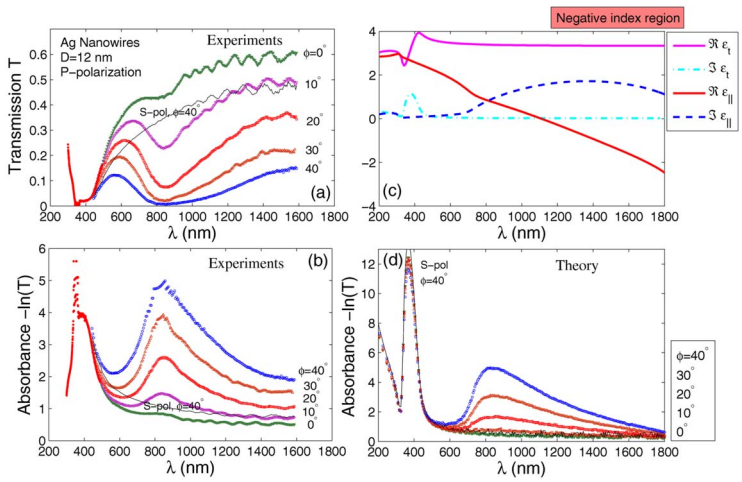

FIG. 2. (Color online) Transmission (a) and absorbance (b) spectra for 12 ± 2 nm diameter Ag nanowires in porous alumina for varying angles of incidence (φ) and with *P* polarization. The solid curve is for *S* polarization and $\varphi = 40°$. The feature at 350 nm is an artifact. The nanotemplate is modeled as consisting of a layer d_1 of porous alumina without nanowire followed by a layer d_2 of nanowires within alumina. This nanotemplate is placed on a glass substrate of 1.5 mm for optical measurements. (c) Anisotropic permittivity of the Ag nanowires in alumina with $\kappa_\perp = 0.75$, $\kappa_\parallel = 95$, and the filling ratio $f = 0.055$. The dielectric constant of amorphous alumina is taken to be 2.25. (d) Calculated absorbance of Ag nanotemplate with $d_1 = 2.9$ μm, $d_2 = 1.1$ μm.

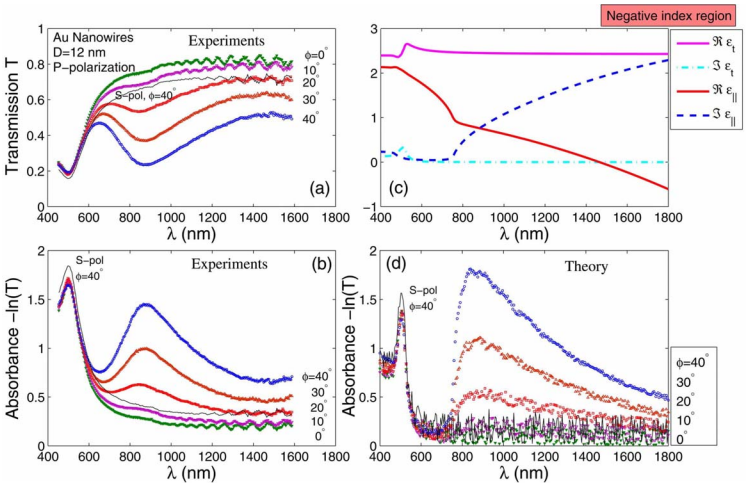

FIG. 3. (Color online) Transmission (a) and absorbance (b) spectra for 12 ± 2 nm diameter Au nanowires in porous alumina for varying angles of incidence (φ) and with P polarization. The solid curve is for S polarization and $\varphi=40°$. The nanotemplate is modeled as consisting of a layer d_1 of porous alumina without nanowire followed by a layer d_2 of nanowires within alumina. This nanotemplate is placed on a glass substrate of 1.5 mm for optical measurements. (c) Anisotropic permittivity of the Au nanowires in alumina with $\kappa_\perp=0.85$, $\kappa_\parallel=60$, and the filling ratio $f=0.04$. The dielectric constant of amorphous alumina is taken to be 2.25. (d) Calculated absorbance of Au nanotemplate with $d_1=3.5$ μm, $d_2=0.5$ μm.

with positive effective permittivity so that the condition for the longitudinal resonance is never realized. Hence this peak is always absent. From the model, this in turn also implies that negative refraction will not be possible under these conditions. The same explanation holds for the P-polarized waves close to normal incidence. However, for large angles of incidence of the P-polarized wave, the electric field oscillations have a component parallel to the wire axis, thus interacting with the longitudinal resonance. Thus, with increasing angle of incidence, the condition for the longitudinal resonance and consequently that for negative refraction is also met.

The corresponding modeling results for the anisotropic permittivity and absorbance are shown in Figs. 2(c) and 2(d). For the calculations, we have used the same parameters (fill ratio, aspect ratio, etc.) corresponding to the templates studied above. Also, optical constants for Ag and aluminum oxide are taken from Ref. 17. Comparing with the experimental results on absorbance, one notes that there is good agreement in peak positions and angle dependence. Also, one notes that for this sample, Re $\varepsilon_\parallel<0$ for wavelengths $\lambda>1100$ nm. Beyond this wavelength, it will behave as a negative index material.[11]

Similar plasmon resonances are observed for Au nanowires with wire diameter 12 ± 2 nm, as shown in Figs 3(a) and 3(b). Here the transverse resonance is seen at 500 nm and is again independent of angle of incidence and polarization direction. The longitudinal resonance is strongly dependent on the incident angle and observed only for P polarization. The longitudinal peak is in the range 845–875 nm and shows a small blueshift for increased angle of incidence. The corresponding modeling results are shown in Figs. 3(c) and 3(d). As in the case of Ag, the optical constants for Au and alumina are taken from Ref. 17. The absorbance calculations are in very good agreement with the experimental results. In this case, the sample will behave like a negative index medium for wavelength, $\lambda>1450$ nm [see Fig. 2(c)].

In conclusion, nanocomposite structures consisting of very high aspect ratio metal nanowires embedded in dielectric have been demonstrated. Detailed transmission studies on such structures reveal the presence of two resonance peaks, the position and peak intensity of which are clearly dependent on the nanocomposite dimensions, filling ratio and the angle of incidence and polarization direction. The results are consistent with a model based on Bruggeman's effective medium theory. The nonlocal effect[18,19] on effective permittivity is small and negligible, which is confirmed in our band structure calculation.[11] The analyses[20] based on Maxwell–Garnett theory failed to predict the window for negative refraction and superlens imaging. Though direct laser writing[21] can also be used to obtain nanorod arrays, the simple fabrication approach used in this study is easily amenable to varying wire dimensions, aspect ratio and fill factor to produce structures which can exhibit negative refraction in the visible wavelength regime. Such structures also demonstrate easy compatibility with micro and nanoscale engineering processes making the development of such devices a feasibility in the near future.

Work supported by NSF CAREER Grant Nos. ECS-0551468, BES-06018892, and DMR-0305360 and Air Force Research Laboratory, Hanscom, MA through Contract No. FA8718-06-C-0045.

[1] V. M. Shalaev, Nat. Photonics **1**, 41 (2007), and references therein.
[2] S. A. Maier, Curr. Nanosci. **1**, 17 (2005).
[3] U. Kreibig and M. Vollmer, *Optical Properties of Metal Clusters* (Springer, Berlin, 1995), Vol. 25.
[4] M. Kerker, *The Scattering of Light and other Electromagnetic Radiation* (Academic, New York, 1969).
[5] C. F. Bohren and D. R. Huffman, *Absorption and Scattering of Light by Small Particles* (Wiley, New York, 1983).
[6] B. McMillan, L. Berlouis, F. R. Cruickshank, and D. Pugh, Appl. Phys. Lett. **86**, 211912 (2005).
[7] V. Podolsky, A. K. Sarychev, E. E. Narimanov, and V. M. Shalaev, J. Opt. A, Pure Appl. Opt. **7**, S32 (2005).
[8] A. Ono and S. Kawata, Phys. Rev. Lett. **95**, 267407 (2005).
[9] V. A. Podolskiy and E. E. Narimanov, Phys. Rev. B **71**, 201101 (2005).
[10] J. Elser, R. Wangberg, V. A. Podolskiy, and E. E. Narimanov, Appl. Phys. Lett. **89**, 261102 (2006).
[11] W. T. Lu and S. Sridhar, Phys. Rev. B **77**, 233101 (2008).
[12] A. Sihvola, *Electromagnetic Mixing Formulas and Applications* (Institution of Electrical Engineers, London, UK, 1999).
[13] V. M. Shalaev, *Nonlinear Optics of Random Media: Fractal Composites and Metal-Dielectric Films* (Springer, Berlin, 1999).
[14] D. R. Smith and D. Schurig, Phys. Rev. Lett. **90**, 077405 (2003).
[15] H. Masuda, H. Yamada, M. Satoh, and H. Asoh, Appl. Phys. Lett. **71**, 2770 (1997).
[16] J. Chunxin and P. C. Searson, Appl. Phys. Lett. **81**, 4437 (2002).
[17] J. H. Weaver, *Optical Properties of Metals* (Fachinformationszentrum, Karlsruhe, Germany, 1981).
[18] A. L. Pokrovsky and A. L. Efros, Phys. Rev. B **65**, 045110 (2002).
[19] M. G. Silveirinha, Phys. Rev. E **73**, 046612 (2006).
[20] R. Atkinson, W. R. Hendren, G. A. Wurtz, W. Dickson, A. V. Zayats, P. Evans, and R. J. Pollard, Phys. Rev. B **73**, 235402 (2006).
[21] C. Reinhardt, S. Passinger, B. N. Chichkov, W. Dickson, G. A. Wurts, P. Evans, R. Pollard, and A. V. Zayats, Appl. Phys. Lett. **89**, 231117 (2006).